

Supplementary information

Clean SiO₂ Atomic Layer Etching based on Physisorption of High Boiling Point-Perfluorocarbon

Dain Sung,^a Hyunwoo Tak,^a Heeju Kim,^a Dongwoo Kim,^a Kyongnam Kim ^{*b} and Geunyoung Yeom ^{*a,c}

^a *School of Advanced Materials Science and Engineering, Sungkyunkwan University, Suwon 16419, Republic of Korea*

^b *School of Advanced Materials Engineering, Daejeon University, Daejeon 34520, Republic of Korea*

^c *SKKU Advanced Institute of Nano Technology (SAINT), Sungkyunkwan University, Suwon 16419, Republic of Korea*

*Corresponding authors.

E-mail addresses: knam1004@gmail.com (K. N. Kim), gyyeom@skku.edu (G. Y. Yeom)

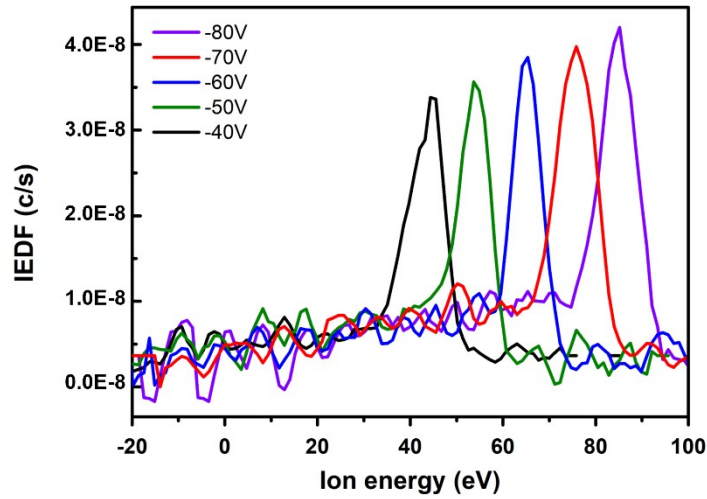


Fig. S1 IEDFs of Ar⁺ ions (input 60 MHz bias voltage of - 40 ~ - 80 V)

Fig. S1 shows the Ar⁺ ion energy distribution function (IEDF) at the center of the substrate using an RFEA (retarding field energy analyzer; Impedance, Semion) with the Ar plasma (bias voltage of -40 ~ -80 V). During the measurements, monoenergetic Ar⁺ ion distributions were observed because a high bias frequency of 60 MHz was used to minimize the energy split of IEDF for anisotropic etching of SiO₂. It is believed that the monoenergetic distribution of the Ar⁺ ions can control the fluorocarbon layer deposited on the SiO₂ and Si₃N₄ precisely during the HBP ALE process.

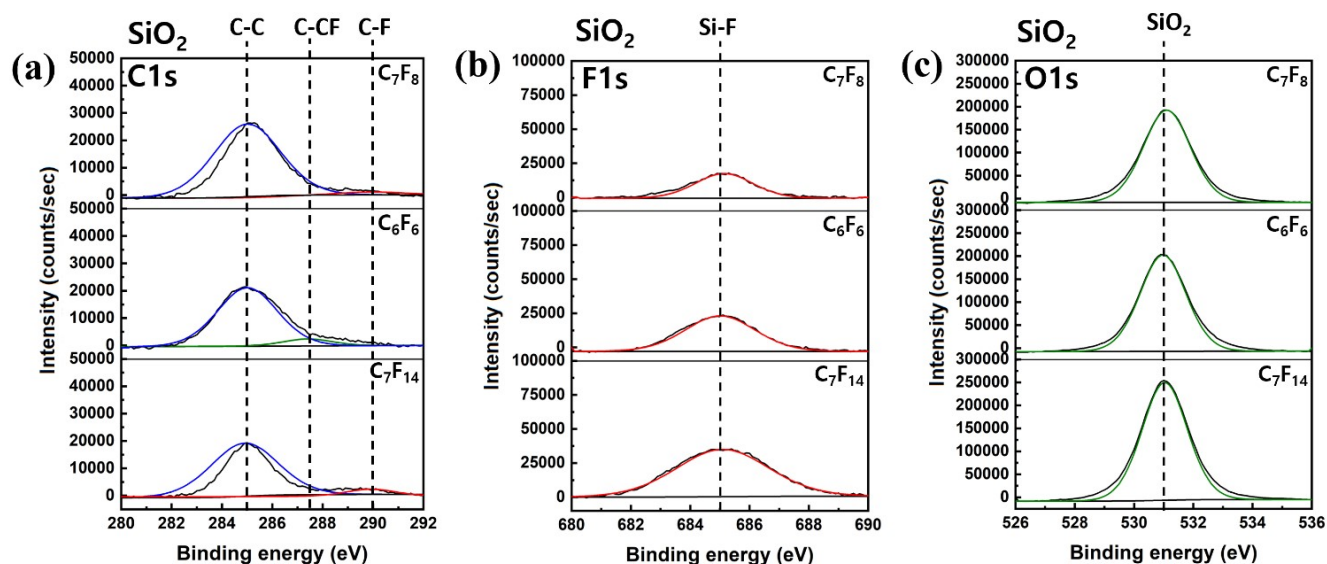


Fig. S2 (a) C1s, (b) F1s, and (d) O1s XPS narrow scan spectra of SiO₂ surface after ALE process (for 70 cycles) using C₇F₁₄, C₆F₆, and C₇F₈ at the optimized process conditions. The temperature of all substrates was maintained at -15 °C.

The binding states of carbon, fluorine, and oxygen on the surfaces of SiO₂ after the ALE processes investigated using XPS. SiO₂ samples were etched at the following conditions; for C₇F₁₄ with the bias voltage of -50 V, for C₆F₆ with bias voltage of -70 V, and for C₇F₈ with the bias voltage of -80 V while the adsorption time and the desorption time were maintained at 10 s and 5 s, respectively. Other process conditions are the same as those in Fig. 3. As shown, no significant differences in bonding states on the etched surfaces of SiO₂ were observed for F and O bonding peaks among different PFC gases except for C bonding states.

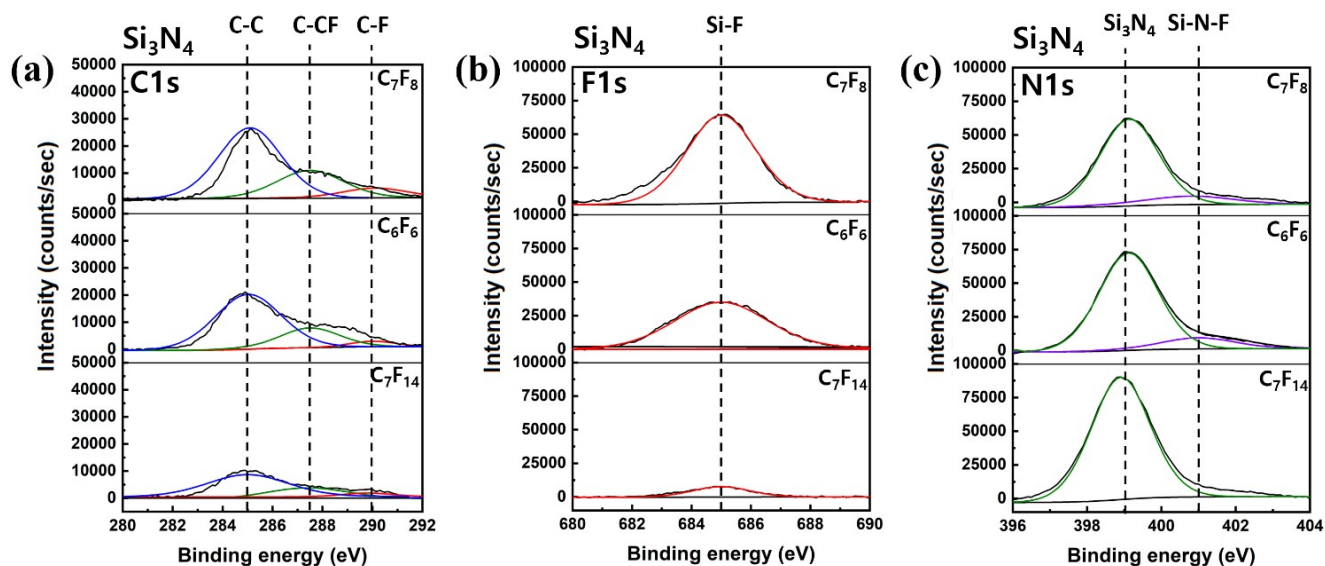


Fig. S3 (a) C1s, (b) F1s, and (d) N1s XPS narrow scan spectra of Si₃N₄ surface after ALE process (for 70 cycles) using C₇F₁₄, C₆F₆, and C₇F₈ at the optimized process conditions. The temperature of all substrates was maintained at -15 °C.

The binding states of carbon, fluorine, and nitrogen on the surfaces of Si₃N₄ after the ALE processes investigated using XPS. Si₃N₄ samples were etched at the following conditions; for C₇F₁₄ with the bias voltage of -50 V, for C₆F₆ with bias voltage of -70 V, and for C₇F₈ with the bias voltage of -80 V while the adsorption time and the desorption time were maintained at 10 s and 5 s, respectively. Other process conditions are the same as those in Fig. 3. As shown, no significant differences in bonding states on the etched surfaces of Si₃N₄ were observed for F and N bonding peaks among different PFC gases except for C bonding states.

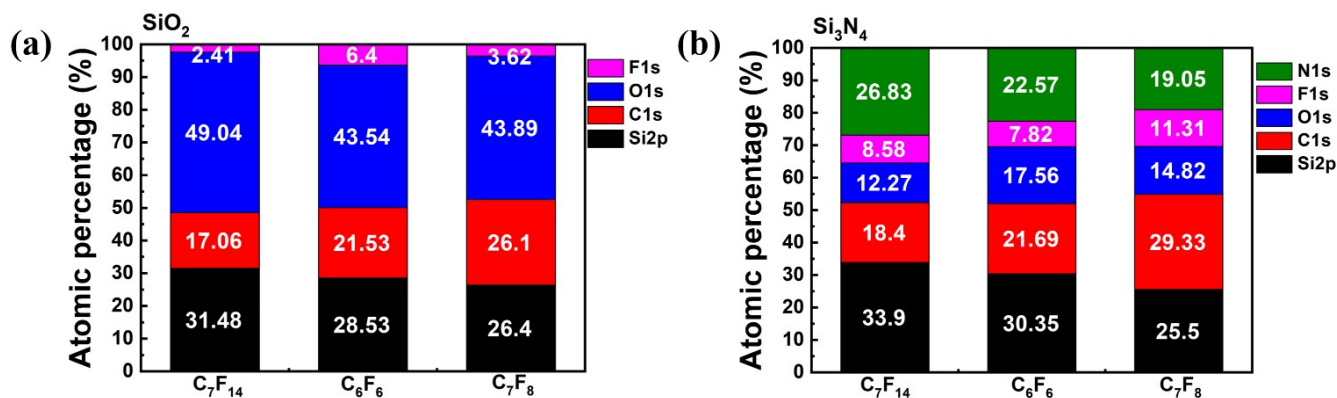


Fig. S4 Atomic percentages of (a) SiO₂ and (b) Si₃N₄ surface measured by XPS after C₇F₁₄, C₆F₆, and C₇F₈-ALE processes (70 cycles) at the optimized process conditions. The temperature of all substrates was maintained at -15 °C.

Atomic percentages of silicon, oxygen, carbon, fluorine, and nitrogen on the surfaces of Si₃N₄ after the ALE processes investigated using XPS. SiO₂ and Si₃N₄ samples were etched at the following conditions; for C₇F₁₄ with the bias voltage of -50 V, for C₆F₆ with bias voltage of -70 V, and for C₇F₈ with the bias voltage of -80 V while the adsorption time and the desorption time were maintained at 10 s and 5 s, respectively. Other process conditions are the same as those in Fig. 3. As shown, the increase of carbon percentage on the etched SiO₂ surface and the increase of carbon and fluorine percentages on the etched Si₃N₄ surface were observed due to the thicker fluorocarbon layer formation in the sequence of C₇F₁₄, C₆F₆, and C₇F₈.

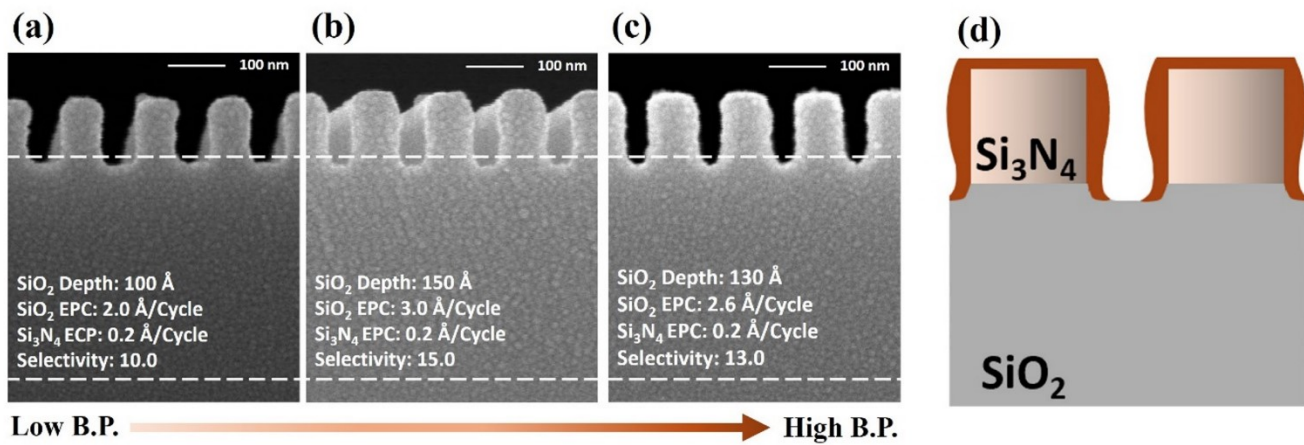


Fig. S5 SEM cross-sectional images of the Si₃N₄ masked SiO₂ sample after the ALE processes for (a) C₇F₁₄, (b) C₆F₆, and (c) C₇F₈ with the optimized process conditions in Fig. 4. (d) Schematic drawing showing a polymer formed at the sidewall of Si₃N₄ mask during the ALE cycles. The number of ALE cycles were 50 cycles. The temperature of all substrates was maintained at -15 °C.

When the ALE processes were performed for 50 cycles using the previously optimized conditions in Fig. 4 using C₇F₁₄, C₆F₆, and C₇F₈, due to the fluorocarbon deposition not only on the top of the Si₃N₄ masked SiO₂ but also on the sidewall of the Si₃N₄ mask, the SiO₂ EPC was decreased to 2.0 Å/cycle for C₇F₁₄, 3.0 Å/cycle for C₆F₆, and 2.6 Å/cycle for C₇F₈, and Si₃N₄ mask was thickened due to the deposition of fluorocarbon layer on the sidewall.